

# Dynamics of cooling in Viscoelastic Granular Gases

Purnendu Pathak<sup>1,\*</sup>, Subhajit Paul<sup>2</sup>, and Subir K. Das<sup>1</sup>

<sup>1</sup>Theoretical Sciences Unit and School of Advanced Materials, Jawaharlal Nehru Centre for Advanced Scientific Research, Jakkur P.O., Bangalore 560064, India

<sup>2</sup>Department of Physics and Astrophysics, University of Delhi, Delhi 110007, India

**Abstract.** We carry out computational study of pattern formation during cooling in assemblies of inelastically colliding granular particles, under force free condition. Typically, in such systems, following a homogeneous cooling phase, a crossover occurs to a phase that is defined by the inhomogeneity in the density field. This inhomogeneity is known to persist for the remaining part of the evolution process, if the coefficient of restitution ( $e$ ) is chosen to be a constant. However, in real situations,  $e$  depends upon the relative velocity of the colliding partners. In this work, we choose a model that mimics this scenario. In addition to presenting results on the pattern dynamics, an important objective of the work is to initiate a study for obtaining a picture on the effectiveness of model parameters.

## 1 Introduction

Granular materials are commonly seen in nature, covering a wide range of lengths. Typical examples include sand particles, food grains and cosmic dust. Unlike molecular gases, the granular particles undergo inelastic collisions and thus, naturally cool with time by losing kinetic energy [1]. We note here that the time ( $t$ )-dependent granular temperature, for  $N$  particles, is defined as [1]  $T(t) = 1/N \sum_{i=1}^N m v_i^2(t)/2$ ,  $v_i$  being the speed of particle  $i$  and  $m$  the mass of each particle. These cooling systems remain out-of-steady-state unless the energy loss is compensated via external supplies. Such evolving systems, under force-free conditions, are referred to as freely cooling granular gases [1]. During the initial stage of cooling, the density remains uniform. This is referred to as the homogeneous cooling state (HCS) [1, 2]. At late times, inhomogeneity appears in the density field [3, 4], alongside the velocity field, showing particle-rich and particle-poor regions, similar to those observed during a vapor-liquid phase transition [3–6]. While there exists rigorous analytical understanding [1, 2] of the temperature decay in the HCS, the knowledge about the inhomogeneous cooling state (ICS) [1, 3, 4] is primarily acquired via computer simulations and dimensional arguments [3–8].

While in a large set of theoretical studies, the value of  $e$ , the coefficient of restitution, is considered to be a constant, for real materials  $e$  typically depends upon the relative velocity ( $\vec{v}_{\text{rel}}$ ) of the colliding partners [9, 10]. Essentially, in such viscoelastic systems [1], higher  $\vec{v}_{\text{rel}}$  leads to inelastic collisions and the collisions are practically elastic for small values of  $\vec{v}_{\text{rel}}$ . The effective coefficient of restitution, in these systems, can be modeled via an expansion [11–15] in  $g_{ij} \equiv |\vec{v}_{\text{rel}} \cdot \hat{n}|$ , with  $\hat{n} = (\vec{r}_i - \vec{r}_j)/|\vec{r}_i - \vec{r}_j|$  being the

direction of the unit vector joining the colliding particles  $i$  and  $j$ . In this work, we focus on the density relaxation, temperature decay and evolution in restitution coefficients in such a class of viscoelastic granular gases. In the HCS, for the constant  $e$  case, the decay of  $T$  follows Haff's cooling law [2]:  $T(t) \sim (1 + t/t_0)^{-2}$ ,  $t_0$  being a time-scale [2, 4]. For a viscoelastic gas, the early time decay is somewhat slower [16]:  $T(t) \sim (1 + t/t_v)^{-5/3}$ . After the system crosses over to the ICS regime,  $T(t)$  deviates from the Haff's law. Certain scaling arguments predict [4, 7, 8, 17]  $T(t) \sim t^{-\theta}$ , with  $\theta = 2d/(d + 2)$ ,  $d$  being the space dimension. The validity of this prediction has been verified in the ICS via numerical simulations, for the constant  $e$  case [5, 7, 8]. Part of the present work is related to corresponding investigation in a model viscoelastic gas with the variation of crucial model parameters.

## 2 Model and methods

We perform numerical simulations using event-driven molecular dynamics [18] (EDMD), during which we keep track of the collision times and the colliding partners for all events. Following a collision, the velocity update equations, obeying the momentum conservation rule, can be written as [18]  $\vec{v}_i = \vec{v}_i - [(1 + e)/2][\hat{n} \cdot (\vec{v}_i - \vec{v}_j)]\hat{n}$ ,  $\vec{v}_j = \vec{v}_j + [(1 + e)/2][\hat{n} \cdot (\vec{v}_i - \vec{v}_j)]\hat{n}$ . Here  $\vec{v}_{i,j}$  and  $\vec{v}'_{i,j}$  are pre- and post-collisional velocities of particles  $i$  and  $j$ , respectively. The (relative) velocity-dependent effective coefficient of restitution for the viscoelastic particles is modeled as [14, 15]

$$e_{\text{eff}} = (1 - e_0) \exp(-|g_{ij}/v_c|^q) + e_0, \quad (1)$$

where  $v_c$  is a cut-off velocity and  $e_0$  is a constant. The value of  $v_c$  is set to unity as this provides a physically relevant velocity scale for the system. This form suggests that

\*e-mail: purnenduju@jncasr.ac.in

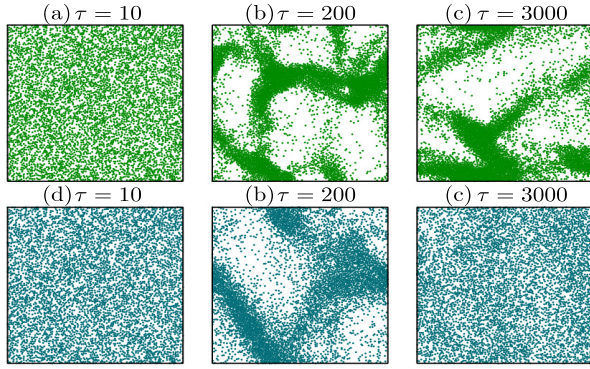


**Figure 1.** (a) – (c): Evolution snapshots for a freely cooling granular gas when  $e$  is fixed at  $0.8$ . (d) – (f): Similar to the top panels but here the snapshots are for the viscoelastic case, with the chosen parameters  $e_0 = 0.8$ ,  $v_c = 1$  and  $\alpha = 1/5$ . For both the cases, the considered system size is  $L = 128$ , with number density of particles being  $0.3$ .

$e_{\text{eff}} \rightarrow 1$ , for  $\vec{v}_{\text{rel}} \rightarrow 0$ , and  $e_{\text{eff}} \rightarrow e_0$ , for high  $\vec{v}_{\text{rel}}$ . This complies with the experimental scenario [9, 10]. While it is possible that [11–13] there exists an optimum value of the exponent  $\alpha$ , studies on the effects of variation of  $\alpha$  (as well as of  $e_0$  and the initial temperature  $T(0)$ ) are limited. Such investigations are of practical relevance [9, 10], in the sense of existence or absence of universality, by considering the fact that even a simple step function like model [16], where above a certain cut-off velocity  $e = e_0 (< 1)$ , and below that it is elastic, i.e.,  $e = 1$ , can produce certain basic properties of viscoelastic particles. For different model varieties the readers may look at Refs. [12, 13]. In this study, we consider wide ranges of values for the parameters  $\alpha$  and  $T(0)$ .

All our simulations (with  $2D$  systems) are performed in square boxes of linear dimension  $L$ , in units of particle diameter  $\sigma (= 1)$ , with the number density  $\rho = 0.3$ . Unless otherwise mentioned, we have used  $L = 256$ ,  $T(0) = 10$  and  $e_0 = 0.8$ . To compare with experiments appropriate units for  $m$ ,  $\sigma$  and  $v$  can be set, e.g., as kg, meter and meter/sec. Initial positions and velocities of the grains were assigned randomly. Periodic boundary conditions are applied in both the directions. We measure time by summing up intervals between “every” two successive collisions. In the literature, for such problems, another measure of time is used, viz., the collision time ( $\tau$ ). Increment of  $\tau$ , by one unit, is related to  $N/2$  number of collisions, with  $N$  being the total number of particles [5, 6]. We present the results as a function of  $t$ , as well as  $\tau$ , after averaging over runs with 50 independent initial configurations.

### 3 Results

We start by showing the time evolution snapshots in Fig. 1. There, for a comparison, we show the corresponding pictures for the case of constant  $e$  as well. See the top panels. Starting from a homogeneous distribution of particles, at  $\tau = 0$ , the density inhomogeneity, relating particle-rich and particle-poor regions, appears due to inelastic colli-

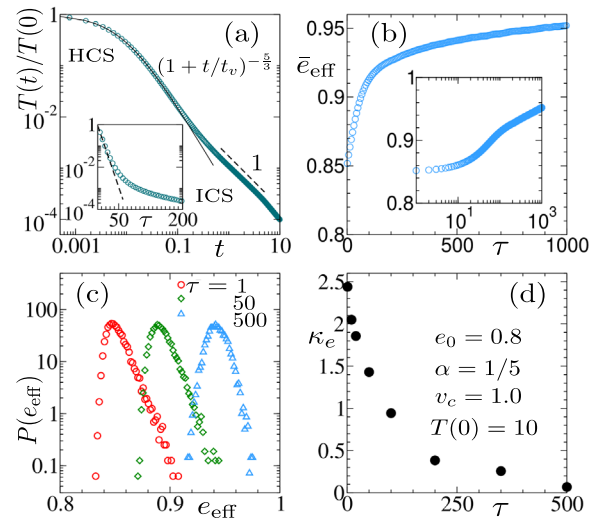


**Figure 2.** (a) Plot of normalized temperature,  $T(t)/T(0)$ , versus  $t$ , for the viscoelastic gas. The solid line corresponds to Haff’s law in the HCS, whereas the dashed line suggests another power-law decay in the ICS with exponent 1. Inset shows the same data but here plotted against the collision time,  $\tau$ . In the HCS, it appears linear, on a semi-log scale, suggesting an exponential decay. (b) Variation of  $\bar{e}_{\text{eff}}$ , as a function of  $\tau$ , for the same system as in (a). Inset shows the same data but here the abscissa is shown in a log scale to display the early time feature. (c) Plot of the distribution  $P(e_{\text{eff}})$ , versus  $e_{\text{eff}}$ , at different times. (d) Plot of kurtosis,  $\kappa_e$ , versus  $\tau$ , for the same set of parameter values.

sions. As seen, the time evolution is quite similar for both of them (constant  $e$  and viscoelastic cases) only until a certain time. For fixed  $e$ , the clusters keep growing [5, 6]. Contrary to that, for the viscoelastic particles, the clustering behavior disappears at a later time, i.e., the system relaxes back to a homogeneous density state, as evident from the snapshot at  $\tau = 3000$ . This can be quantified via the calculation of equal time two-point correlations [5] in the density field. With time, in the constant  $e$  case, the decay of the correlation function becomes slower, suggesting continuous growth of the length scale [6]. For the viscoelastic case, the length scale will show a non-monotonic behavior, within which the later time decay would suggest decorrelation in the density field due to re-entrance into the homogeneous phase. These multiple regimes of relaxation, in the latter case, may be tunable by varying the parameters  $T(0)$ ,  $e_0$  and  $\alpha$ . In the remaining part of the paper, we investigate these.

In Fig. 2(a) we show the decay of normalized temperature,  $T(t)/T(0)$ , versus  $t$ , for  $e_0 = 0.8$ ,  $v_c = 1$  and  $\alpha = 1/5$ . At initial times, we see that the Haff-like law is valid with [16]  $T(t) \sim (1 + t/t_v)^{-5/3}$ . After a certain time, the decay of  $T(t)$ , however, deviates from the HCS behavior, marking the onset of a crossover to the ICS. In this region, decay of temperature approximately obeys  $T(t) \sim t^{-1}$ , similar to that [4–6] with constant  $e$ . However, at a much later time, the system goes to a homogeneous state again, as seen in Fig. 1(f), and the energy decay deviates from  $t^{-1}$  behavior (not shown for extended period). The inset shows the same decay as a function of the collision time  $\tau$ .

To capture the microscopic details of the re-entrant behavior of the density relaxation, towards a homogeneous phase, via an inhomogeneous route, we show in Fig 2(b) the time dependence of  $\bar{e}_{\text{eff}}$ . For each  $\tau$ , the value of  $\bar{e}_{\text{eff}}$  has been calculated as the mean of the distribution of  $e_{\text{eff}}$  obtained from its  $N/2$  values. For given  $v_c$ ,  $T(0)$  and  $\alpha$ ,  $e_{\text{eff}}$  shows a monotonic increase towards 1. This is effectively due to decreasing  $g_{ij}$ , because of parallelization of velocities, owing to reduction in normal components of relative velocities via inelastic collisions. See Eq. (1). As  $e_{\text{eff}} \rightarrow 1$ , the collisions become increasingly elastic, leading to the breakdown of clusters that, in turn, leads to the homogeneous density distribution. Further details on this evolution are provided below.

In Fig. 2(c) we plot the distribution,  $P(e_{\text{eff}})$ , of  $e_{\text{eff}}$ , from a few values of  $\tau$ . These values of  $\tau$ , in ascending order, are chosen in such a way that they correspond to HCS, ICS, and the final homogeneous regime, respectively. At early times, the distributions are non-Gaussian, though the velocities may obey Gaussian form. However, at much later times, the distributions tend to be Gaussian. Also, as  $\tau$  increases the mean shifts to higher values, asymptotically moving toward unity, the elastic limit. To have a quantitative understanding of this transformation of the distribution, we calculate the corresponding kurtosis ( $\kappa_e$ ), defined as [19]  $\kappa_e = \langle (e_{\text{eff}} - \bar{e}_{\text{eff}})^4 \rangle / \langle (e_{\text{eff}} - \bar{e}_{\text{eff}})^2 \rangle^2 - 3$ . Departure from  $\kappa_e = 0$  corresponds to a deviation from Gaussian. In Fig. 2(d) we plot  $\kappa_e$ , versus  $\tau$ . Starting from a much higher value,  $\kappa_e$  moves towards 0. This happens when  $\bar{e}_{\text{eff}}$  moves towards unity, and density tends to be homogeneous. Here we note that the values of  $\alpha$ ,  $e_0$  and  $T(0)$  take part in determining the value of  $e_{\text{eff}}$  and thus, its distribution, which in turn determines the rate of energy dissipation. Thus, it is useful to investigate the evolutions of energy and  $\kappa_e$  with the variations of these parameters.

In Fig. 3(a) we plot  $T(\tau)/T(0)$ , versus  $\tau$ , for a few different values of  $\alpha$ , by fixing other parameters at values same as in Fig. 2. Data for different  $\alpha$  values show consistency in the HCS. Furthermore, this common early period behavior appears consistent with the Haff-like law, as demonstrated in the inset. However, the crossover, to the ICS, occurs earlier for a higher value of  $\alpha$ . We plot  $\bar{e}_{\text{eff}}$ , versus  $\tau$ , in Fig. 3(b), for the same set of values of  $\alpha$  as in Fig. 3(a). The data for  $\alpha = 0.2$  clearly appears slowest in approach to the elastic limit. To probe the behavior at early times, we present the same data sets on a log-log scale, in the inset. Note here that at early times, for some value of  $g_{ij}$ , say, when  $> v_c$ , the factor  $\exp(-|g_{ij}|/v_c)^\alpha$  will be smaller for a larger  $\alpha$ . This corresponds to a smaller value of  $\bar{e}_{\text{eff}}$ , closer to  $e_0$ . See Eq. (1). This can be appreciated from the early parts of the plots in the inset. A lower value of the coefficient of restitution should lead to larger dissipation, which eventually will lead to lowering, as well as parallelization, of velocities faster and correspondingly the value of  $g_{ij}$ . Then a fall in the value of  $g_{ij}$  makes  $\bar{e}_{\text{eff}}$  larger, leading the collisions to be more elastic. Thus,  $\bar{e}_{\text{eff}}$  reaches unity earlier for a higher value of  $\alpha$ , even though the starting value is smaller. For a quantification of the dependencies of related time, on  $\alpha$ , we look at the behavior of a characteristic time scale ( $\tau_c$ ) at which the collisions

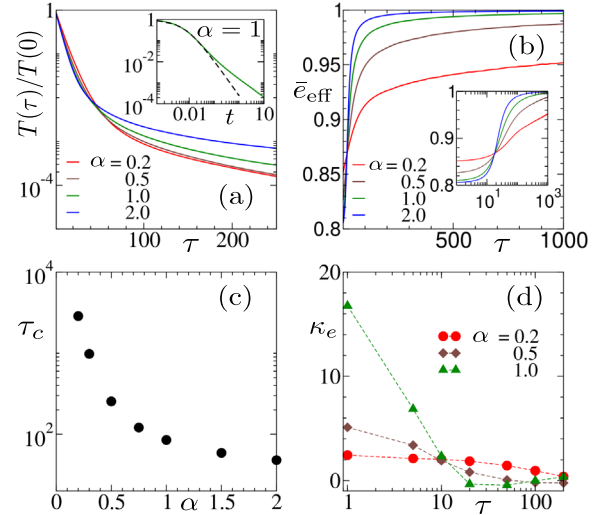


**Figure 3.** (a) Log-linear plots of  $T(\tau)/T(0)$ , versus  $\tau$ , for a few values of  $\alpha$ , keeping the other parameters same as in Fig. 2. Inset shows a log-log plot, for  $\alpha = 1.0$ , versus  $t$ . There the dashed line corresponds to Haff's law. (b) Plots of  $\bar{e}_{\text{eff}}$ , versus  $\tau$ , for different  $\alpha$  values, as in (a). The inset shows the same data sets, now the abscissa being presented in a log scale. (c) Plot of a characteristic time scale  $\tau_c$ , at which  $\bar{e}_{\text{eff}}$  crosses a certain value, viz., 0.97, versus  $\alpha$ . (d) Plot of kurtosis  $\kappa_e$ , versus  $\tau$ , for different values of  $\alpha$ .

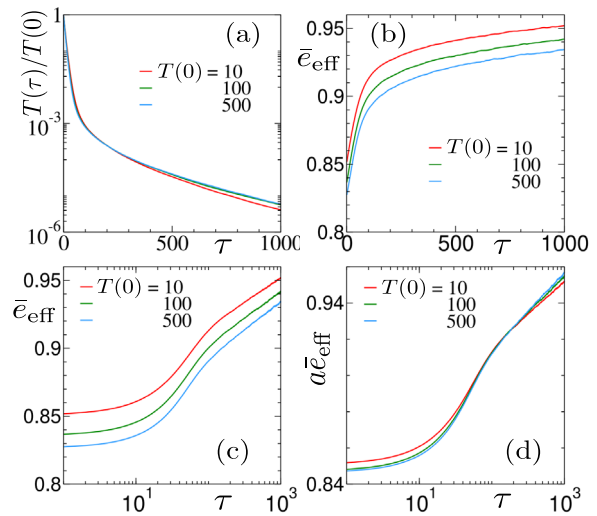


**Figure 4.** (a) Plots of the decay of  $T(\tau)/T(0)$ , versus  $\tau$ , on a semi-log scale, for a few choices of the initial temperature,  $T(0)$ , with  $\alpha = 1/5$ ,  $v_c = 1$  and  $e_0 = 0.8$ . (b) Plots of  $\bar{e}_{\text{eff}}$ , versus  $\tau$ , for the same choices of  $T(0)$ . (c) Same as (b) but here a semi-log scale is used. (d) Same as (c), now with a  $T(0)$ -dependent prefactor in the ordinate.

become nearly elastic, viz., when  $\bar{e}_{\text{eff}}$  reaches a value 0.97. A plot of this quantity is shown in Fig. 3(c), as a function of  $\alpha$ . Furthermore, analogous to Fig. 2(d), we plot  $\kappa_e$ , versus  $\tau$ , in Fig. 3(d), now for different choices of  $\alpha$ . In each of the cases,  $\kappa_e$  changes from a much higher value towards 0. The approach is quicker for higher  $\alpha$ .

Next we investigate the effects of varying  $T(0)$  in Fig. 4. While this may be equivalent to varying  $v_c$ , it should be noted that  $v_c$  sets a velocity scale. Thus, we refrain from varying this quantity. In Fig. 4 (a), we plot  $T(\tau)/T(0)$ , versus  $\tau$ , on a semi-log scale. General character is same, irrespective of the values of  $T(0)$ , except for minor variation in crossover time. In Fig. 4(b) we plot  $\bar{e}_{\text{eff}}$ , versus  $\tau$ , for the same set of values of  $T(0)$ . The ones having the lower  $T(0)$  is reaching the elastic limit earlier. This can be explained along the same line as done for the case of variation in  $\alpha$ . For better visualization of different regimes, same set of plots are shown again in part (c), on a semi-log scale. They appear reasonably parallel to each other, throughout. Thus, it was possible to obtain a collapse by a simple transformation via introduction of a  $T(0)$ -dependent prefactor ‘ $a$ ’ in the ordinate. See Fig. 4(d). This collapse implies that basic evolution properties remain largely unchanged with the variation of  $T(0)$ . However, such a collapse is not possible against the variation in  $\alpha$ , implying a complex role of  $\alpha$  in the modeling of viscoelastic particles. We note that the variation in  $e_0$ , like in  $T(0)$ , also does not change the qualitative behavior in the evolution of  $e_{\text{eff}}$ . However, in future it will be interesting to find out long-time effects via extended simulations.

## 4 Conclusion

In this work, we consider a freely cooling granular gas with impact velocity-dependent coefficient of restitution [14, 15] that mimics collisions in real situations [9, 10]. Starting from a homogeneous density phase, the system shows a re-entrant behavior at a later time, via intermediate inhomogeneous cooling state in which particle-rich and particle-poor regions appear. For quantitative understanding we explore evolutions in energy and coefficient of restitution. A non-Gaussian distribution of the latter quantity, in the initial homogeneous phase, tends towards a Gaussian one in the late time uniform density phase. Thus, there exists fundamental difference between the two homogeneous phases. We have studied the effects of certain model parameters on such evolution. In future we would like to simulate larger systems over longer periods to come to a better conclusion by discarding the effects due to finite size. Such future study will also include quantities related to the evolution of velocity distribution. It will be interesting to bring connection between this and that for  $e_{\text{eff}}$ .

## References

- [1] N. Brilliantov, T. Poschel, Kinetic Theory of Granular Gases (Oxford University Press, Oxford, 2004)
- [2] P.K. Haff, Grain flow as a fluid-mechanical phenomenon, *J. Fluid Mech.* **134**, 401–430 (1983). [10.1017/S0022112083003419](https://doi.org/10.1017/S0022112083003419)
- [3] I. Goldhirsch, G. Zanetti, Clustering instability in dissipative gases, *Phys. Rev. Lett.* **70**, 1619 (1993). [10.1103/PhysRevLett.70.1619](https://doi.org/10.1103/PhysRevLett.70.1619)
- [4] X. Nie, E. Ben-Naim, S. Chen, Dynamics of freely cooling granular gases, *Phys. Rev. Lett.* **89**, 204301 (2002). [10.1103/PhysRevLett.89.204301](https://doi.org/10.1103/PhysRevLett.89.204301)
- [5] S.K. Das, S. Puri, Kinetics of inhomogeneous cooling in granular fluids, *Phys. Rev. E* **68**, 011302 (2003). [10.1103/PhysRevE.68.011302](https://doi.org/10.1103/PhysRevE.68.011302)
- [6] S. Paul, S.K. Das, Dynamics of clustering in freely cooling granular fluid, *Europhys. Lett.* **108**, 66001 (2014). [10.1209/0295-5075/108/66001](https://doi.org/10.1209/0295-5075/108/66001)
- [7] S. Paul, S.K. Das, Ballistic aggregation in systems of inelastic particles: Cluster growth, structure, and aging, *Phys. Rev. E* **96**, 012105 (2017). [10.1103/PhysRevE.96.012105](https://doi.org/10.1103/PhysRevE.96.012105)
- [8] S. Paul, S.K. Das, Dimension dependence of clustering dynamics in models of ballistic aggregation and freely cooling granular gas, *Phys. Rev. E* **97**, 032902 (2018). [10.1103/PhysRevE.97.032902](https://doi.org/10.1103/PhysRevE.97.032902)
- [9] C.V. Raman., The photographic study of impact at minimal velocities, *Phys. Rev.* **12**, 442 (1918). [10.1103/PhysRev.12.442](https://doi.org/10.1103/PhysRev.12.442)
- [10] L. Labous, A.D. Rosato, R.N. Dave, Measurements of collisional properties of spheres using high-speed video analysis, *Phys. Rev. E* **56**, 5717 (1997). [10.1103/PhysRevE.56.5717](https://doi.org/10.1103/PhysRevE.56.5717)
- [11] R. Ramírez, T. Pöschel, N.V. Brilliantov, T. Schwager, Coefficient of restitution of colliding viscoelastic spheres, *Phys. Rev. E* **60**, 4465 (1999). [10.1103/PhysRevE.60.4465](https://doi.org/10.1103/PhysRevE.60.4465)
- [12] A. Bodrova, N. Brilliantov, Granular gas of viscoelastic particles in a homogeneous cooling state, *Physica A Stat. Mech. Appl.* **388**, 3315 (2009). <https://doi.org/10.1016/j.physa.2009.04.040>
- [13] A.K. Dubey, A. Bodrova, S. Puri, N. Brilliantov, Velocity distribution function and effective restitution coefficient for a granular gas of viscoelastic particles, *Phys. Rev. E* **87**, 062202 (2013). [10.1103/PhysRevE.87.062202](https://doi.org/10.1103/PhysRevE.87.062202)
- [14] M. Shinde, D. Das, R. Rajesh, Violation of the prod law in a freely cooling granular gas in one dimension, *Phys. Rev. Lett.* **99**, 234505 (2007). [10.1103/PhysRevLett.99.234505](https://doi.org/10.1103/PhysRevLett.99.234505)
- [15] M. Shinde, D. Das, R. Rajesh, Coarse-grained dynamics of the freely cooling granular gas in one dimension, *Phys. Rev. E* **84**, 031310 (2011). [10.1103/PhysRevE.84.031310](https://doi.org/10.1103/PhysRevE.84.031310)
- [16] T. Pöschel, N.V. Brilliantov, T. Schwager, Long-time behavior of granular gases with impact-velocity dependent coefficient of restitution, *Physica A Stat. Mech. Appl.* **325**, 274 (2003). [10.1016/S0378-4371\(03\)00206-1](https://doi.org/10.1016/S0378-4371(03)00206-1)
- [17] G.F. Carnevale, Y. Pomeau, W.R. Young, Statistics of ballistic agglomeration, *Phys. Rev. Lett.* **64**, 2913 (1990). [10.1103/PhysRevLett.64.2913](https://doi.org/10.1103/PhysRevLett.64.2913)
- [18] M.P. Allen, D.J. Tildesley, Computer Simulation of Liquids (Oxford University Press, Oxford, 1991)
- [19] K. Pearson, IX. mathematical contributions to the theory of evolution.—xix. second supplement to a memoir on skew variation, *Phil. Trans. R. Soc. Lond. Series A* **216**, 429 (1916). [10.1098/rsta.1916.0009](https://doi.org/10.1098/rsta.1916.0009)